Selected for a Viewpoint in *Physics*
PRL **102,** 146602 (2009) PHYSICAL REVIEW LETTERS week ending 10 APRIL 2009

Electronic Refrigeration of a Two-Dimensional Electron Gas

J. R. Prance,* C. G. Smith, J. P. Griffiths, S. J. Chorley, D. Anderson, G. A. C. Jones, I. Farrer, and D. A. Ritchie

Cavendish Laboratory, J. J. Thomson Avenue, Cambridge CB3 0HE, United Kingdom

(Received 12 November 2008; published 6 April 2009)

Measurements are presented of a device designed to cool a 6 μm^2 region of 2D electron gas using quantum dots. Electrostatic effects are found to be significant in the device, and a model that accounts for them is developed. At ambient electron temperatures above 120 mK the results are consistent with the model and the base temperature of the cooled region is estimated. At an ambient electron temperature of 280 mK, the 6 μm^2 region is found to be cooled below 190 mK. Below 120 mK the results deviate from predictions, which is attributed to reduced electron-electron scattering rates.

DOI: 10.1103/PhysRevLett.102.146602 PACS numbers: 72.20.Pa, 73.23.Hk, 73.63.Kv

Extreme cooling of 2D electron gases (2DEGs) is necessary to study many fundamental physical phenomena, such as the Kondo effect or fractional quantum Hall states. However, cooling such electron gases is problematic since the dominant mechanism for thermalizing with the host lattice, acoustic-phonon scattering, is weak. The 2DEG is commonly found to be heated above the lattice temperature by electrical noise introduced via measurement wiring. The lowest reported electron temperatures when cooling with a dilution refrigerator are around 10 mK [1,2] and achieved by carefully filtering all electrical connections to the sample. Temperatures as low as 4 mK have also been obtained in a lattice cooled to 2 mK using a nuclear demagnetization refrigerator [3]. While successful, such arrangements are complex and limited to cooling the electrons only to the lattice temperature.

Edwards *et al.* [4] suggested a scheme for electronic refrigeration of a 2DEG—the "quantum dot refrigerator" (QDR)—that allows cooling even below the lattice temperature. In achieving this, the weak electron-phonon coupling is an asset rather than a limitation. The QDR uses energy dependent tunneling through two quantum dots with well-resolved single-particle states to cool an isolated 2DEG (see Fig. 1). Previously, the superconducting energy gap has been used in a similar way to cool electron gases in metals [5,6], heavily doped silicon [7], and metal charge islands [8]. It has also been suggested that low-dimensional electron gases could be used to increase the efficiency of thermionic cooling [9]. Previous experiments on thermal effects in semiconductor quantum dots have largely focused on thermopower and self-heating measurements [10–12]. The QDR has the potential to achieve efficient refrigeration using similar and relatively well-established experimental techniques.

In this Letter we present measurements of a QDR designed to cool a 6 μm^2 electron gas. Significant electrostatic interactions are observed in the device, which were previously neglected [4]. We develop a model to account for these and, by comparing its predictions to the results, we infer the temperature of the cooled 2DEG.

Figure 2 shows a device lithographically identical to the one measured. NiCr/Au gates were patterned on the surface of a GaAs/AlGaAs heterostructure using electron beam lithography. A 2DEG 90 nm below the surface, with a carrier density of $n = 1.37 \times 10^{11}$ cm^{-2}, is contacted by annealed AuGeNi contacts. The surface gates can define an enclosed, central 2DEG region with quantum dots to the left (dot A) and above (dot B). The right dot is unused in this experiment. The central region, of area $A \approx 6$ μm^2, is expected to hold $nA \approx 8000$ electrons. The energy separation between their states will be approximately $(2\pi\hbar^2/Am^*) = 1.2$ μeV. This is always less than $k_B T_E$ (T_E is the ambient electron temperature in the device), so this region can be treated as a Fermi gas.

The device was cooled in a dilution refrigerator with a base temperature of 40 mK. All electrical connections pass through 100 kHz low-pass RC filters thermally anchored to the mixing chamber. The current from the source was measured with an electrometer. The ambient electron temperature (T_E) was determined at various mixing chamber temperatures by fitting to nonlinear measurements of Coulomb blockade in dot A [13].

The central region and two quantum dots were characterized separately. Both dots were found to have charging

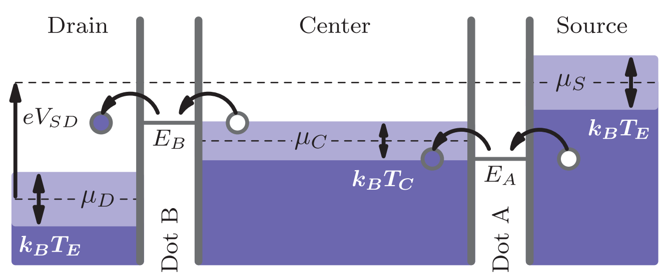

FIG. 1 (color online). QDR energies in the cooling regime. Thermal broadening in the three 2DEGs (source, center and drain) is shown by the light shading around their electrochemical potentials (μ_S, μ_C, μ_D). The net flow of an electron from source to drain removes an energy $E_B - E_A$ from the center. E_A (E_B) is the ground state addition energy of dot A (B).

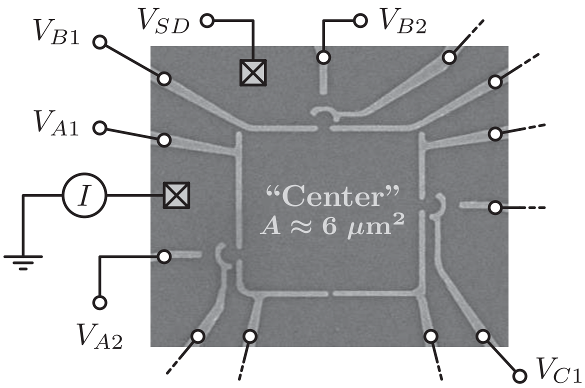

FIG. 2. SEM image of a typical device. Schematic measurement setup is also shown.

energies of approximately 1.5 meV and first excited states always at least 125 μeV above the ground state. The central region was also found to have a significant charging energy of approximately 100 μeV [see Fig. 3(a)]. In addition, a capacitive coupling was observed between the central region and the dots: adding one electron to a dot shifted the central region potential (μ_C) by 30 μeV. Neither this backaction nor the Coulomb blockade of the center were included in the original QDR proposal [4]. Their importance is discussed later.

Having characterized the components, the behavior of the full QDR was investigated. A bias voltage (V_{SD}) greater than $k_B T_E/e$ is needed to ensure that, when cooling, states in the source are full and states in the drain are empty at the dot energies. A bias of 75 μV was used, being less than the charging energy of the center, and the excited state energies of both dots. Thus, the energy levels of the device resemble the ideal case in Fig. 1.

Current through the QDR is measured as a function of the gate voltages V_{A2} and V_{B2} (see Fig. 2), to which the dot energies, E_A and E_B, are linearly related. Current only flows when both E_A and E_B lie between the source and drain potentials (μ_S and μ_D). This gives rise to points of

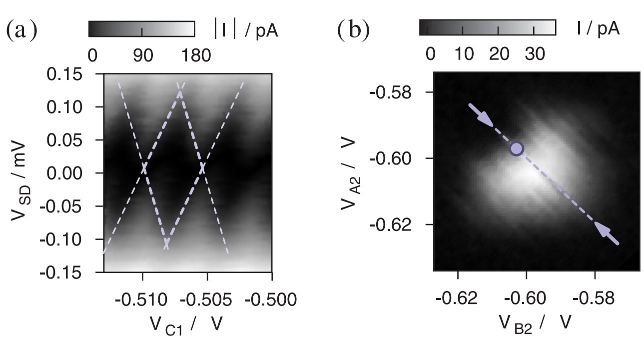

FIG. 3 (color online). (a) Bias spectroscopy of the central region with dots A and B undefined. Dotted lines emphasize the weak Coulomb blockade. Absolute current is plotted for clarity (the sign follows the bias direction as expected.) (b) Point of conduction through the QDR with a bias $V_{SD} = 75\ \mu$V.

conduction in the V_{A2}-V_{B2} plane, which repeat on a square grid with a period set by the dot charging energies, and have a size set by V_{SD}. Figure 3(b) shows a typical measurement of one such conduction point.

Cooling of the central region is expected around the region of the conduction point indicated by the circle in Fig. 3(b). Along the dotted line, E_A and E_B are moving in opposite directions and pass half way between μ_S and μ_D. At the bottom right, current begins to flow as E_A drops below μ_S and E_B exceeds μ_D. At the top left, the flow of current is suppressed as E_A drops below E_B. In between, the central 2DEG is cooled when $E_A \lesssim E_B$, and is heated when $E_A > E_B$.

To ascertain how far the central 2DEG is being cooled, the obvious method would be to determine its temperature using a third quantum dot. With an applied bias a dot can be an independent thermometer of either of its leads and, with a sufficiently small tunnel coupling, this measurement would be essentially noninvasive. Indeed it has been shown that the coupling may be made arbitrarily small when using single electron counting techniques [14]. However in the presence of a significant electrostatic coupling between the dot and the measured 2D system, as in our device, the scheme is not feasible: μ_C changes depending on the charge state of an adjacent dot.

As an alternative to an independent thermometer, we instead use the current through the QDR itself to infer the temperature in the center. The line shape of the current along the dotted line in Fig. 3(b) should be determined by both T_E and the central region temperature (T_C). Its exact shape will be nontrivial, but can be predicted.

We calculate the current through a QDR and the associated cooling (or heating) of the center from the charge-state probability distribution for three charge islands in series, as determined by the appropriate master equation [4,15,16]. We allow E_A, E_B and μ_C to depend on the charge state according to a model capacitor network, as used for triple dots [17]. The model therefore includes the effect of both the central region Coulomb blockade and the back-action on μ_C from the dot charges.

For equilibrium, the net heat flow into the center must be zero. The model converges to this solution by varying T_C to balance the QDR cooling (or heating) with two other processes. The first is electron to acoustic-phonon coupling which is predicted to have a power density of $\sigma(T_C^5 - T_L^5)$, where T_L is the lattice temperature, and $\sigma \approx$ 40 fW μm^{-2} K^{-5} for the carrier density in this device [4,18,19]. The second process is heating from electrons tunneling through the lifetime-broadened, Lorentzian tails of the dot states, which is expected to be a fundamental limitation of QDR performance [4]. We model this heat leak as being due to uniform tunnel barriers connecting the center to the source and drain in parallel to the dots. The heat flow ($\dot{Q}_B$) depends on the electrical conductance of the barriers (G_B), the voltage drop (V) and temperature difference ($\Delta T = T_C - T_E$) across them, and the mean temperature [$\bar{T} = (T_E + T_C)/2$], according to the Wiedemann-Franz law [10]:

$$\dot{Q}_B = -2G_B\left[\left(\frac{k_B^2\pi^2}{3e^2}\right)\bar{T}\Delta T - \frac{V^2}{2}\right].$$

Figure 4(a) shows an example of the line shape of the current predicted by this model, and the corresponding profile of T_C. The lowest T_C is 130 mK, which is designated the "base temperature" (T_B). The most noticeable feature in the current, compared to the noncooling case (also shown), is a strong asymmetry. This is a consequence of the QDR altering the temperature of the center. The degree of asymmetry is related to T_B, as shown by Fig. 4(b). In this plot, the right side of the peak changes little because it is primarily determined by thermal broadening in the reservoirs, provided $k_B T_C < eV_{SD}/2$.

The main limitation of the model described above is the assumption of fast electron-electron scattering. This is the mechanism by which the occupation of states in the cooled 2DEG reequilibrates to a Fermi distribution after the injection of an out-of-equilibrium carrier. This rate decreases with temperature [20], and the model will fail when it drops below the rate of carrier injection into central region states. We expect to then enter a regime where transport is suppressed by the slow scattering, except when the two dots inject and remove electrons at the same energy. With no electrostatic interactions this would occur when $E_A = E_B$. In this device, however, the condition may be satisfied in many ways and we would expect to observe a collection of peaks in current.

Measurements of the QDR were made at several temperatures. Three examples are shown in Fig. 5. The plots show the current as V_{A2} and V_{B2} are varied simultaneously

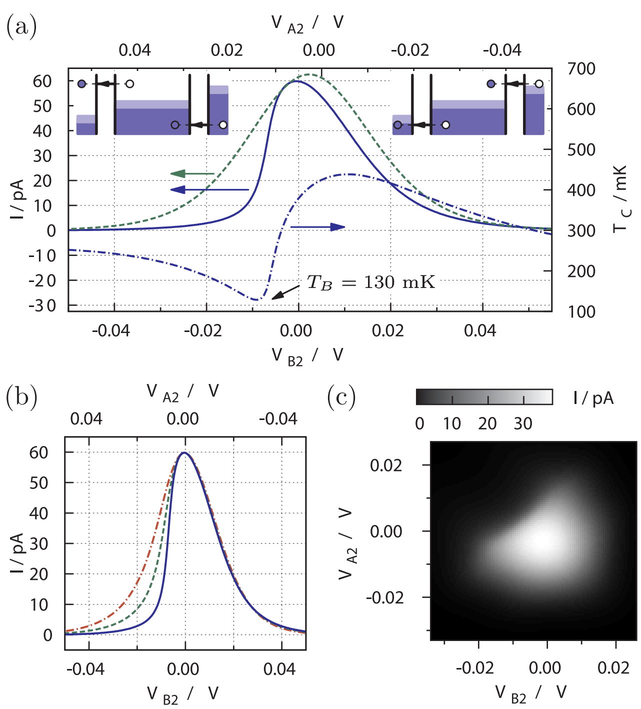

FIG. 4 (color online). (a) Solid line is a typical predicted current as E_A and E_B are moved in opposite directions. Insets are energy levels, as in Fig. 1, at the left and right sides of the plot. Dot-dashed line is the corresponding central region temperature. Parameters are $T_E = 300$ mK, $T_L = 200$ mK, $V_{SD} = 75$ μV and $G_B = 80$ nS. Dashed line is the predicted current for the same parameters, but calculated without converging to equilibrium; i.e. $T_C = T_E$. (b) Line shapes with different electronic heat leaks ($\dot{Q}_B$), giving base temperatures of $T_B = 130$ mK (solid), 215 mK (dashed line) and 300 mK (dot-dashed line). (c) Simulation of the measurement in Fig. 3(b).

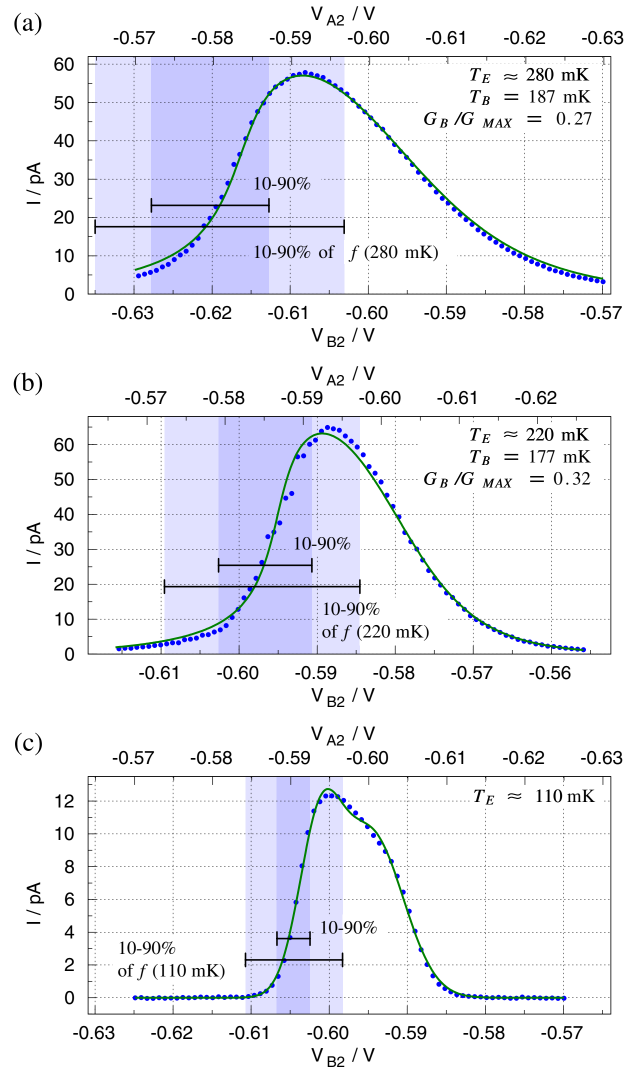

FIG. 5 (color online). Measurements of the QDR current while varying V_{A2} and V_{B2}. $V_{SD} = 75$ μV. The mixing chamber temperature and ambient electron temperature vary between plots. In (a) and (b) the solid line is a fit to the model described in the text. The fitted G_B is given as a fraction of the peak conductance ($G_{MAX} = \max(I)/V_{SD}$). In (c) the solid line shows the best fit to the sum of two Gaussian peaks.

to follow a line diagonally through the center of a conduction point, as with the dotted line in Fig. 3(b). All data in Fig. 5 are the average of repeated measurements taken over several hours to reduce noise.

Line shapes with a distinct asymmetry were observed at all temperatures without requiring considerable effort to tune the device. Furthermore, the sharp sides of the peaks in current were significantly narrower than should be possible if the central 2DEG were thermally broadened by $k_B T_E$. The shaded ranges in Fig. 5 compare the width of these sharp edges with the width of Fermi functions at the appropriate temperatures.

For the two highest temperature results in Fig. 5 we find that the measured line shapes are well described by our QDR model. In Fig. 5(a) the line shape is consistent with a maximum reduction in the central region electron temperature by 93 mK from an ambient 280 mK, corresponding to a cooling power of approximately 0.5 fW. The result in Fig. 5(b) is consistent with a smaller temperature reduction of only 43 mK. This is likely due to the device operating with less optimal tuning during this measurement, rather than the lower T_E.

When fitting calculated line shapes to the data, most parameters of the model were determined by independent measurements. All capacitances were found by separate characterisation of the dots, the central region and the full QDR. The position of each conduction point in V_{A2} and V_{B2} was found by fitting the measured current [as in Fig. 3(b)] to a simulation [as in Fig. 4(c)]. We also determine the minimum μ_C in this way, via the particular shape of the conduction point. The final result is then fitted by varying only the total tunnel rate of the system and the size of the electronic heat leak ($\dot{Q}_B$), via G_B, which determines the line shape asymmetry and T_B.

For the lowest temperature result, shown in Fig. 5(c), the model fits the data poorly. Instead, the data are better described by the sum of two Gaussian peaks. The reason for this is not understood in detail but may be due to the transition into the regime of low electron-electron scattering. Given the current, this suggests that the scattering time of a carrier with an energy within 37.5 μeV (half the bias) of μ_C is greater than 13 ns. Similarly, as the higher-temperature measurements are well described by the model, the scattering time at these temperatures should be less than 7 ns. Both these bounds are consistent with predictions and measurements of large energy transfer electron-electron scattering rates [20,21].

In conclusion, we have demonstrated the feasibility of electronic cooling of a 2DEG using energy selective tunneling through quantum dots. A model of the device, which includes electrostatic effects, explains the data well at temperatures above 120 mK, and the data is consistent with cooling of the isolated 2DEG by over 90 mK in the best case. This is almost certainly not the limit of such a device and we propose three improvements. First, to use more controllable dots so that the device may be optimised for lowest base temperatures. Second, increase the size of the cooled region, increasing the number of states per unit energy and moving the crossover to the low electron-electron scattering regime to lower temperatures. Third, increase the total capacitance of the cooled region to reduce electrostatic effects and enable the use of an independent thermometer. Ultimately this may allow a QDR to be used as a general platform for extra-low-temperature measurements, with devices operating within it probed by noninvasive charge sensors.

We thank C. Ford, A. Thorn, and K. Cooper for useful discussions. Computing resources were provided by CamGrid. This work was funded by EPSRC (UK). I. F. acknowledges financial support from Toshiba.

*jp376@cam.ac.uk

[1] R. M. Potok *et al.*, Nature (London) **446**, 167 (2007).
[2] Y. C. Chung, M. Heiblum, and V. Umansky, Phys. Rev. Lett. **91**, 216804 (2003).
[3] J. S. Xia *et al.*, Physica (Amsterdam) **280B**, 491 (2000).
[4] H. L. Edwards, Q. Niu, and A. L. de Lozanne, Appl. Phys. Lett. **63**, 1815 (1993); H. L. Edwards *et al.*, Phys. Rev. B **52**, 5714 (1995).
[5] M. Nahum, T. M. Eiles, and J. Martinis, Appl. Phys. Lett. **65**, 3123 (1994).
[6] M. M. Leivo, J. P. Pekola, and D. V. Averin, Appl. Phys. Lett. **68**, 1996 (1996).
[7] A. M. Savin *et al.*, Appl. Phys. Lett. **79**, 1471 (2001).
[8] O. P. Saira *et al.*, Phys. Rev. Lett. **99**, 027203 (2007).
[9] A. N. Korotkov and K. K. Likharev, Appl. Phys. Lett. **75**, 2491 (1999).
[10] M. Switkes *et al.*, Appl. Phys. Lett. **72**, 471 (1998).
[11] A. A. M. Staring *et al.*, Europhys. Lett. **22**, 57 (1993).
[12] R. Scheibner *et al.*, Phys. Rev. Lett. **95**, 176602 (2005).
[13] D. V. Averin, A. N. Korotkov, and K. K. Likharev, Phys. Rev. B **44**, 6199 (1991).
[14] K. MacLean *et al.*, Phys. Rev. Lett. **98**, 036802 (2007).
[15] R. L. Kautz, G. Zimmerli, and J. M. Martinis, J. Appl. Phys. **73**, 2386 (1993).
[16] D. V. Averin and K. K. Likharev, *Mesoscopic Phenomena in Solids* (Elsevier Science, Amsterdam, 1991), Chap. 6, p. 173.
[17] D. Schröer *et al.*, Phys. Rev. B **76**, 075306 (2007).
[18] N. J. Appleyard *et al.*, Phys. Rev. Lett. **81**, 3491 (1998).
[19] B. K. Ridley, Rep. Prog. Phys. **54**, 169 (1991).
[20] L. Zheng and S. Das Sarma, Phys. Rev. B **53**, 9964 (1996).
[21] A. G. Huibers *et al.*, Phys. Rev. Lett. **81**, 200 (1998).